Quasi-Classical Trajectory Study of the Vibrational and Translational Effects on the O(P-3) + CD4 Reaction

ARTICLE *in* THE JOURNAL OF PHYSICAL CHEMISTRY A · MAY 2014

Impact Factor: 2.69 · DOI: 10.1021/jp502414e · Source: PubMed

1 AUTHOR:

Joaquin Espinosa-Garcia
Universidad de Extremadura
141 PUBLICATIONS **2,171** CITATIONS

SEE PROFILE

THE JOURNAL OF PHYSICAL CHEMISTRY A

Article

pubs.acs.org/JPCA

Quasi-Classical Trajectory Study of the Vibrational and Translational Effects on the $O(^3P) + CD_4$ Reaction

Joaquín Espinosa-Garcia*

Dpto. Química Física, Universidad de Extremadura, 06071 Badajoz, Spain

ABSTRACT: The effects of vibrational excitation and translational energy, connected to mode selectivity and Polanyi's rules, are important issues in dynamics studies. To analyze these effects on the $O(^3P) + CD_4$ reaction, an exhaustive dynamics study was performed using quasi-classical trajectory calculations on a full-dimensional analytical potential energy surface. The independent excitation of the C−D symmetric or asymmetric stretch modes leads to reactions with similar reaction cross sections and product scattering distributions, mode selectivity being discarded. Finally, translational energy raises the reactivity more effectively than an equal amount of energy in vibration, thus indicating that for this "central barrier" reaction it is not clear how to apply the venerable Polanyi's rules. The strong coupling between vibrational modes is responsible for this behavior, which seems to be the general tendency in polyatomic systems.

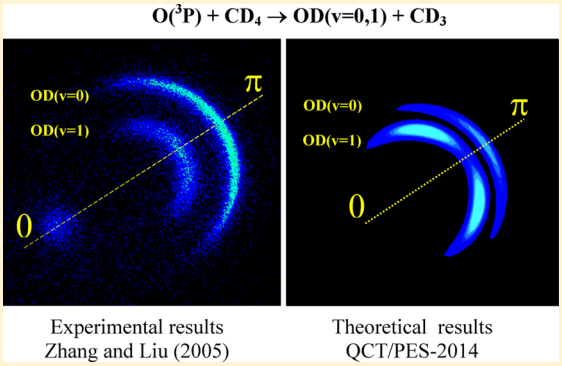

1. INTRODUCTION

The effects of vibrationally excited molecules on reaction dynamics have attracted the attention of many dynamics researchers, and concepts such as bond and mode selectivity and Polanyi's rules[1] are closely related. On the basis of atom + diatom systems, Polanyi found that, for a "late" barrier (product-like), reactant vibrational energy can be more effective than an equal amount of translational energy, while for "early" barrier (reactant-like) the reverse is true. However, nothing is said about reactions with a "central" barrier (i.e., neither reactant-like nor product-like). In the simplest case, atom + diatom, where only one vibrational mode is present, these effects are straightforward to predict, but in the case of polyatomic systems, the larger number of vibrational modes involved makes the direct application of these concepts difficult, due to the possibility of energy flow between them, an effect known as intramolecular vibrational redistribution (IVR).[2]

Thus, in polyatomic systems at the same total energy, we found[3,4] that for the $OH + NH_3$ reaction with an early barrier the translational energy is more effective in driving the reaction, while in the $Cl + NH_3$ reaction with a late barrier, the vibrational energy is more effective. Therefore, these results represent an extension of Polanyi's rules to polyatomic systems. However, when we analyzed the $F + CH_4$ reaction and an isotopomer analogue, $F + CH_2D_2$, which present a clear early barrier, we found contradictory results.[5,6] Thus, while the $F + CH_4$ fulfils the Polanyi's rules, the $F + CH_2D_2$ reaction contradicts them. This finding is unexpected from the direct application of Polanyi's rules, indicating that in polyatomic reactions their application is neither straightforward nor always valid. In that work, we interpreted the results based on the strong coupling between modes in the entrance channel before the collision, related to IVR. Contradictory results have been also found by other authors. For instance, in the experimental study of the $Cl + CHD_3$ reaction (late barrier), Liu and co-workers[7] found contradictory results. So, while the bending mode excitation is only slightly more effective than an equal amount of translational energy, unexpectedly the C−H stretch excitation is not more effective. The strong coupling between vibrational modes, previously predicted theoretically,[8,9] was argued to interpret the experimental results. More recently, theoretical studies[10,11] of the $O(^3P) + CH_4$ reaction, which presents a central barrier, showed that translational energy is more effective in driving the reaction, while experimentally Zhang and Liu[12] found that, contrary to the theoretical predictions, bend-excited methane does not increase reactivity. For the $O(^3P) + CHD_3$ reaction, Wang and Liu[13] found significant vibrational enhancement when the C−H is vibrationally excited by one quantum. However, this study was not performed at the same total energy, and so the comparison is not valid. Possibly, near the threshold of the ground state reaction, additional translational energy will always be more effective than vibrational energy.[14] Recently, Jiang and Guo[15] studied the relative efficacy of vibrational and translational energy excitation in promoting atom−diatom reactivity and proposed the sudden vector projection (SVP) model as an alternative to venerable Polanyi's rules.

In sum, in polyatomic systems the application of Polanyi's rules is more complex[16] than a simple extrapolation of those rules from simpler atom−diatom reactions.

To analyze these dynamics problems we focused our attention on the $O(^3P) + CD_4(\nu) \rightarrow OD(\nu) + CD_3(\nu)$ gas-

Received: March 10, 2014
Revised: May 1, 2014
Published: May 2, 2014

   dx.doi.org/10.1021/jp502414e | J. Phys. Chem. A 2014, 118, 3572−3579

phase reaction, which is slightly endothermic (ΔE_R = 5.8 and $\Delta H_{R,0K}$ = 3.1 kcal mol^{-1},), with a central barrier. For the O(^{3}P) + CH_4 reaction[17] and its isotopomer analogues, we recently developed an analytical full-dimensional potential energy surface, named PES-2014.[17] In that work[17] we found that the quasi-classical trajectory calculations (QCT) reproduce the experimental evidence: concave-up excitation function, cold OH product rotovibrational distributions, and backward scattering distribution.

The main objectives of the present work were 2-fold: first, to analyze the effects of the reactant $CD_4(\nu)$ vibrational excitations on O(^{3}P) + $CD_4(\nu)$ → OD(ν) + $CD_3(\nu)$ reaction dynamics; and second, to test the difficulties involved in the application of Polanyi's rules to polyatomic reactions.

The article is structured as follows: Section 2 briefly presents the PES-2014, while section 3 gives the computational details. Section 4 presents the dynamics results, and finally, the conclusions are presented in section 5.

2. POTENTIAL ENERGY SURFACE

A complete description of PES-2014 was given in an earlier paper[17] to describe the O(^{3}P) + CH_4 reaction and its isotopomer analogues and so will not be repeated here. In brief, the functional form is given by

$$V = V_{stretch} + V_{harm} + V_{op} + V_{vdw} \quad (1)$$

where $V_{stretch}$ consists of four London−Eyring−Polanyi-type stretching terms, V_{harm} represents the valence bending terms for each valence angle in methane, V_{op} describes the out-of-plane motion of methyl, and V_{vdw} is a van der Waals term to describe the intermediate complexes in the entrance and exit channels. In addition a series of switching functions are included to allow the smooth change from pyramidal CH_4/CD_4 to planar CH_3/CD_3 product in the hydrogen abstraction reaction. PES-2014 depends on 41 adjustable parameters, which were fitted to ab initio calculations at the CCSD(T) = FULL/aug-cc-pVQZ level. The barrier height and reaction energy are, respectively, 14.1 and 5.8 kcal mol^{-1}, reproducing benchmark calculations.[18] In addition the intermediate complexes in the entrance and exit channels are also well reproduced. Figure 1 plots schematically the variations in potential energy along the hydrogen abstraction reaction path for PES-2014, together with other theoretical values for comparison. Compared with the recent Czako−Bowman (CB) surface,[18] PES-2014 is more rigid for describing the system in such a large configuration space, and simpler because it depends on only 41 parameters. However, the main advantage of this PES is that not only the energy obtained analytically but also the first energy derivatives, i.e., the gradients, which is a very important feature in dynamics (classical, quasi-classical, and quantum mechanical) calculations. Finally, we tested[17] its accuracy and we found that in general the PES-2014 reproduces reasonably well the ab initio information used as input in the fit.

The PES-2014 harmonic vibrational frequencies of reactants and products are listed in Table 1 for the O(^{3}P) + CD_4 reaction, where ν_1 (triply degenerate), ν_2, ν_3 (doubly degenerate), and ν_4 (triply degenerate) are, respectively, the asymmetric stretching, the symmetric stretching, the bending, and the umbrella modes of CD_4. The individual excitation by one quantum of these modes adds extra energy to the reactants, from 2.9 kcal mol^{-1} for the lowest mode (ν_4) to 6.5 kcal mol^{-1} for the highest stretch mode (ν_1).

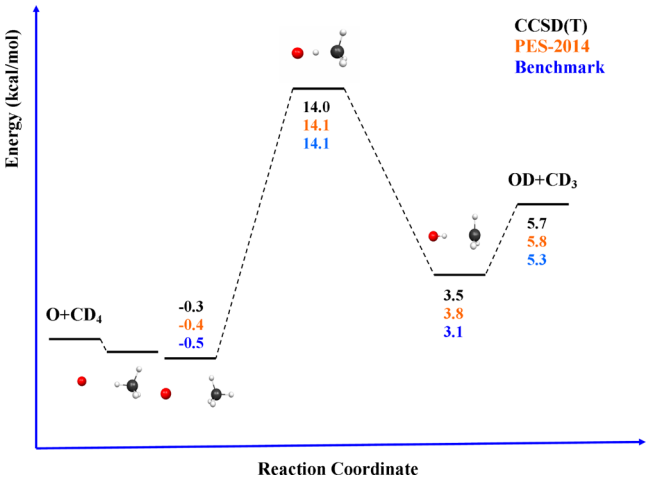

Figure 1. Schematic profile of the potential energy surface along the reaction path. CCSD(T), CCSD(T)=FULL/aug-cc-pVQZ//CCSD-(T)=FC/cc-pVTZ single-point level from ref 16; PES-2014, using the analytical surface developed in ref 16; benchmark, accurate relative energies obtained at the all-electron CCSDT(Q)/complete-basis-set quality from ref 17.

Table 1. Harmonic Vibrational Frequencies (in cm^{-1}) with PES-2014[a]

CD_4	CD_3	OD
2295 (t) (ν_1)	2417(e) (ν_1)	2760 (ν_1)
2074 (ν_2)	2171 (ν_2)	
1060 (e) (ν_3)	11014(e) (ν_3)	
1011(t) (ν_4)	450 (ν_4)	

[a] CD_4: ν_1, ν_2, ν_3, and ν_4 correspond, respectively, to the asymmetric stretch, symmetric stretch, bending, and umbrella modes.

3. COMPUTATIONAL DETAILS

3.1. Initial Conditions. On the basis of the PES-2014 surface, QCT calculations were performed using the VENUS96 code.[19,20] The accuracy of the calculations was checked by the conservation of total energy and total angular momentum. The initial separation between the reactant centers of mass is 10.0 Å, and the integration step is 0.01 fs. The trajectories were stopped when the interatomic C−O distance was 11.0 Å.

We independently consider the $CD_4(\nu)$ in the vibrational ground-state and each mode vibrationally excited by one quantum, in the collision energy range 8.0−20.0 kcal mol^{-1}. For each case, we run 100 000 trajectories with a maximum value of the impact parameter, b_{max}, in the range 0.8−2.3 Å, increasing with the collision energy. In total, about 1.6 × 10^6 trajectories were run, where the rotational energies were obtained by thermal sampling at 298 K from a Boltzmann distribution. For each vibrational state, CD_4 (ν_i = 0,1, i = 1−4), and collision energy, the b_{max} value is obtained running 10 000 trajectories and increasing the value of the b parameter until no reactivity was found. This represents an additional computational cost.

3.2. Final Conditions. The zero-point energy (ZPE) problem represents a serious difficulty in QCT dynamics calculations. The integral cross section is calculated using two different approaches to this problem: (i) HB-All, histogram binning where all trajectories are considered in the analysis of the results without ZPE constraint; and (ii) HB-DZPE, histogram binning where only the trajectories that lead to

dx.doi.org/10.1021/jp502414e | J. Phys. Chem. A 2014, 118, 3572−3579

both products having a vibrational energy above their ZPE are included. In addition, and contrary to the previously analyzed histogram binning (HB) approaches in which all trajectories contribute equally with weight unity, in the Gaussian binning procedure each trajectory is weighted by a Gaussian, where the weights are obtained based on the final vibrational actions (GB approach)[21] or based on the total vibrational energy of the products (1GB approach).[22] In this article we have used only the 1GB approach because in polyatomic systems where the number of vibrational modes is large, the GB approach needs a practically prohibitive number of trajectories to reach the same level of convergence as with the standard binning (HB) procedure.

Once we obtain the rotational and vibrational numbers of the products, in the histogramatic approach they are rounded, i.e., numbers between 0.5 and 1.5 are assigned to a quantum number of 1. Finally, the differential cross section (DCS) of the OD product is obtained by the Legendre moment method.[23]

3.3. Intramolecular Vibrational Redistribution Calculations. The intramolecular vibrational redistribution (IVR) before the collision between reactants was calculated using a modified version[24] of VENUS96. In order to maintain the orientation of the reference equilibrium geometry in the body fixed frame, a rotation and translation of the reactants is necessary. The computational details were developed in the original work[24] or in a recent paper by our group,[3] and so they will not be repeated here.

For the IVR calculation, we run 1000 trajectories for each vibrational state, CD_4 (ν_i = 0,1, i = 1−4). As we analyze the behavior before collision between reactants, the previous initial conditions were modified to ensure that no interaction between them takes place. Thus, we increase the initial separation between the reactant centers of mass to 15.0 Å, and the maximum impact parameter, b_{max}, to 10.0 Å. With these initial conditions we ensure asymptotic trajectories. Finally, the energy of each vibrational mode was averaged for all trajectories at each time. The variation in each normal mode's average energy with time shows the internal flow of energy between normal modes in the $CD_4(\nu)$ reactant, and it can be denoted as "intrinsic" IVR. Note that this energy flow is different from the mode−mode coupling along the reaction path (Coriolis-like terms, eq 4)[25] because the first occurs in the reactant channel previous to the collision and the second shows the energy flow during the reactive collision.

4. RESULTS AND DISCUSSION

4.1. Ground-State Excitation Function. For the CD_4 vibrational ground-state, Figure 2 plots the QCT excitation function on the PES-2014 surface for the energy range 8.0−20.0 kcal mol^{-1} together with the QCT data[10] on the CB surface[18] for comparison. First, this function shows typical threshold behavior of the reactions with barrier, increasing with collision energy. Given that the adiabatic barrier is 11.5 kcal mol^{-1}, all reactivity below this value is artificial because QCT calculations are classical in nature, and no reactivity is allowed below this barrier (tunnelling effect). The shape of the excitation function presents a concave-up collision energy dependency. This shape reflects a relatively tight-bend transition state structure, C−D′−O angle, and this behavior can be explained by the venerable angle-dependent line of center (ADLOC) model. A similar concave-up behavior was found for the CH_4 reaction.[17] In comparing our QCT results with other theoretical results on a different PES (CB), we found excellent agreement in all energy ranges, with differences less than 15%. This result strongly contrasts with the greater differences found for the isotopomer analogue $O(^3P)$ + CH_4 reaction (Figure 2, dashed lines), which were more than 200%. Taking into account that the adiabatic energetic thresholds (using the PES-2014 surface) of CH_4 and CD_4 are 10.2 and 11.5 kcal mol^{-1}, respectively (vertical dashed and solid lines in Figure 2), a diminution of the reactivity for the CD_4 reaction is expected. This behavior is only clearly shown for the PES-2014 surface, while the CB surface shows very similar cross sections for both reactions.

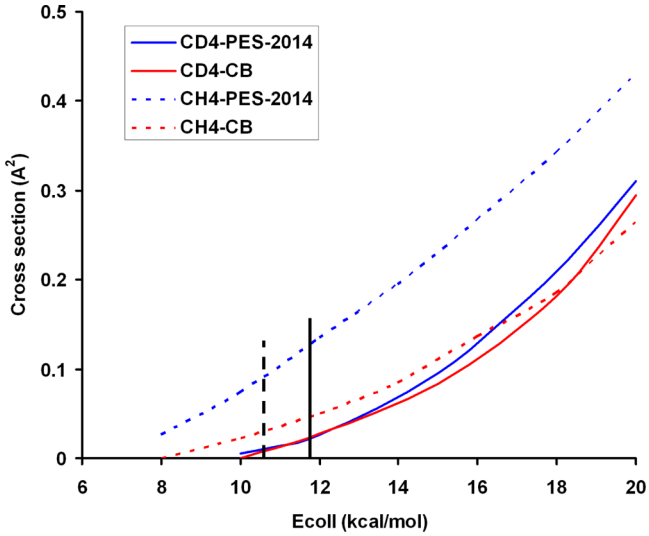

Figure 2. Reaction cross section (Å^2) as a function of the collision energy (kcal mol^{-1}). Comparison of QCT values using the PES-2014 and CB surfaces. Solid lines: $O(^3P)$ + CD_4 reaction. Dashed lines: $O(^3P)$ + CH_4 reaction. The vertical lines are the adiabatic energetic thresholds (PES-2014) for both reactions.

4.2. Role of Vibrational Excitation on Reactivity. The reaction cross sections for the vibrational excitations, CD_4 (ν_i = 1, i = 1−4), with respect to the vibrational ground-state, CD_4 (ν_i = 0 i = 1−4), are listed in Table 2, at collision energy of 15.0 kcal mol^{-1}. In all cases, CD_4 (ν_i = 1, i = 1−4), vibrational excitation increased reactivity by factors 2.0−1.3, where the effect of the CD stretching modes (ν_1 and ν_2) is larger. When the DZPE criterion is considered, the tendency is the same, but the enhancement is larger, 5.1−2.6.

Table 2. QCT Reaction Cross Sections with Respect to O + CD_4 Vibrational Ground-State (gs) on the PES-2014 Surface at Collision Energy of 15.0 kcal mol^{-1}, for Different $CD_4(\nu)$ Vibrational Excitations[a]

	σ_v/σ_{gs}
CD_4 vibrational mode excited	15.0 kcal mol^{-1}
ν_1 (asymm. stretch)	1.71 (5.07)
ν_2 (symm. stretch)	2.00 (5.00)
ν_3 (bending)	1.43 (2.73)
ν_4 (umbrella)	1.33 (2.65)

[a]Values correspond to the HB-All approach, and values in parentheses correspond to the HB-DZPE approach. Maximum error bar ±0.1.

To understand this behavior, Figure 3 plots the reaction path curvature, $\kappa(s)$ (eq 2)[26]

dx.doi.org/10.1021/jp502414e | J. Phys. Chem. A 2014, 118, 3572−3579

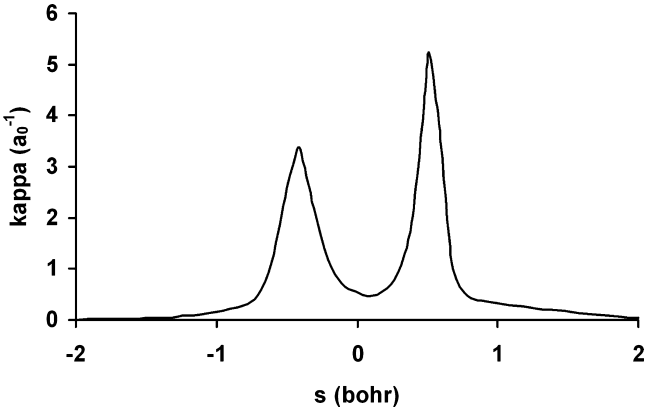

Figure 3. Reaction path curvature, κ, as a function of reaction coordinate, s.

$$\kappa(s) = \left(\sum [B_{i,F}(s)]^2\right)^{1/2} \quad (2)$$

where $B_{i,F}(s)$ is the term measuring the coupling between the normal mode i and the reaction coordinate F,

$$B_{i,F}(s) = -\sum_{l\gamma=1}^{N} \frac{d\nu_{l\gamma}(s)}{ds} c^{i}_{l\gamma}(s) \quad (3)$$

where $\nu_{l\gamma}(s)$ is the $l\gamma$ component of the normalized gradient vector, and $c^{i}_{l\gamma}(s)$ is the $l\gamma$ component of the eigenvector for mode i. So, the larger the $B_{i,F}(s)$ term, the larger the flow of energy between the mode i and F, i.e., excitation of this mode would greatly enhance the reactivity. Figure 3 shows two sharp peaks. The first, in the entrance channel, is due to strong coupling of the reaction coordinate to the CD symmetric stretch, $B_{i,F} = 3.32a_0^{-1}$ at the maximum of κ at $s = -0.423a_0$. The umbrella and the CD asymmetric stretch modes also contribute, though to a lesser extent ($B_{i,F} = 0.58a_0^{-1}$ and $0.29a_0^{-1}$). Therefore, with this naïve mode-selective picture one would expect a priori that excitation of these modes might enhance reactivity. The second peak, in the exit channel ($s = +0.513a_0$), is higher than the first. This is due to the coupling of the reaction coordinate to the OD stretch, which has $B_{i,F} = 5.20a_0^{-1}$, with small contributions from the CD asymmetric mode ($B_{i,F} = 0.12a_0^{-1}$) and umbrella mode ($B_{i,F} = 0.58a_0^{-1}$). Again, this naïve picture suggests that these product modes appear vibrationally excited.

This analysis of the reaction path curvature, however, does not explain the effect of the bending mode on reactivity, which is not coupled to the reaction coordinate. To understand this effect we shall analyze the coupling between modes during the reaction, $B_{i,i'}(s)$ (eq 4)

$$B_{i,i'}(s) = \sum_{l\gamma=1}^{N} \frac{dc^{i}_{l\gamma}(s)}{ds} c^{i'}_{l\gamma}(s) \quad (4)$$

which measures the energy flow between the vibrational modes i and i' in the reactive process. Unlike the intrinsic IVR analyzed in section 3.3, this term shows the collision-induced IVR. We find coupling between bending and umbrella modes in the entrance channel, which explains the transfer of energy between these modes and the effect of excitation of the bending mode on reactivity.

In sum, we found that all modes in CD_4 increase reactivity with respect to the vibrational ground state, more importantly for the stretching modes. These results agree with the recent theoretical values by Czako et al.[10] and reproduce the experimental evidence,[13] where it is noted that little rate-promotion was observed by exciting the bending modes of methane.

4.3. Differential Cross Sections. The product angular distributions at this collision energy, 15.0 kcal mol^{-1}, are analyzed for the different $CD_4(\nu)$ excited vibrational states, comparing the results with recent theoretical[10] and experimental[12] data. This dynamics property is very sensitive to the quality of the PES.

The differential cross sections (DCS) obtained using the Legendre moment method,[23] of the OD product with respect to the incident oxygen atom, are plotted in Figure 4. The

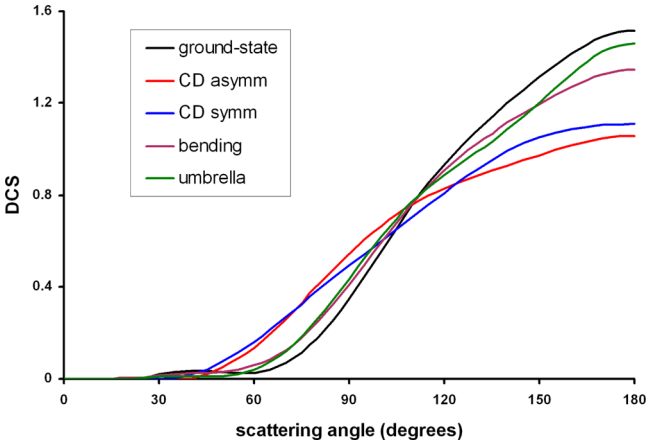

Figure 4. QCT product angular distributions at collision energy of 15.0 kcal mol^{-1} using the PES-2014 surface for OD product (with respect to the incident O) for different $CD_4(\nu)$ vibrational excited states.

scattering angles show a backward behavior, which is independent of the initial vibrational excitation. These findings indicate a direct rebound reaction mechanism. This behavior reproduces the QCT results[10] on the CB surface and the experimental evidence,[12] which measured the ground-state and the bending excitation.

In addition, Zhang and Liu[12] also measured experimentally the DCSs for the OD($\nu = 0$) and OD($\nu = 1$) products in the $O(^3P) + CD_4$ reaction at collision energy of 12.5 kcal mol^{-1}, where both products present backward distribution. The QCT results on the PES-2014 surface at the same collision energy are plotted in Figure 5 and compared with the experiment. The QCT results are consistent with the experiment for both states, although the theoretical results show a less backward character for the OD($\nu = 1$) state. A more complete theory/experiment comparison can be reached by representing the doubly differential cross section, $d^2\sigma/[d\omega \cdot d\cos(\vartheta)]$, in center-of-mass polar coordinates (ω,θ) (Figure 6). Both OD($\nu = 0,1$) states show backward scattering, thus reproducing the experimental evidence,[12] although as was noted previously the QCT OD ($\nu = 1$) state presents a less backward character.

4.4. Mode Selectivity. *4.4.1. CD Symmetric and Asymmetric Comparison: An Example of Coupling Modes.* In section 4.2 (eq 2, Figure 3) we found that the reaction coordinate is strongly coupled to the CD symmetric stretch mode (ν_2) and presents a weak coupling with the CD asymmetric stretch mode (ν_1). With this naïve mode-selective picture, a great difference in reactivity between the two stretch

dx.doi.org/10.1021/jp502414e | J. Phys. Chem. A 2014, 118, 3572−3579

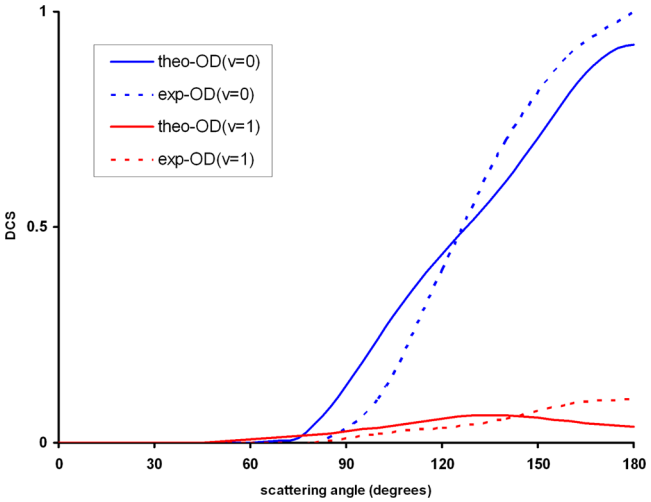

Figure 5. Product angular distributions for OD(ν = 0,1) product from the CD_4(ν = 0) state at collision energy of 12.5 kcal mol^{-1}. Solid lines: QCT results using the PES-2014 surface. Dashed lines: Experimental data from ref 12. For a direct comparison, both sets of data are scaled to the same area for each vibrational state.

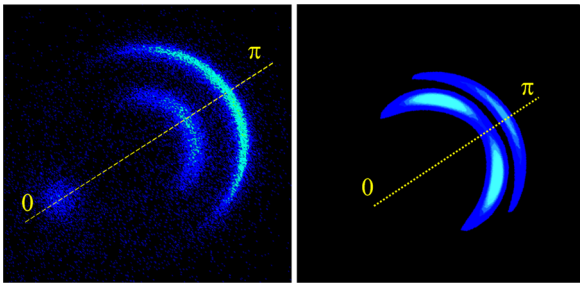

Figure 6. Polar scattering three-dimensional surface plot of the CM scattering angle-velocity distribution, $P(\omega,\theta)$, of the title reaction at collision energy of 12.5 kcal mol^{-1}. Left panel: Experimental results from ref 12. Right panel: QCT theoretical results from this work.

mode excitations could be expected. However, the QCT dynamics results show similar reactivity for both modes (ν_1 and ν_2) (Table 2). To understand this apparent contradiction we shall analyze the intrinsic IVR. Figure 7 plots the temporal evolution of the energy available in different modes for the ground-state CD_4 reactant (ν = 0, panel a), and for the excited CD asymmetric (ν_1 = 1, panel b) and CD symmetric (ν_2 = 1, panel c) stretch modes. The QCT results show an energy flow between modes even in the vibrational ground-state, CD_4(ν =0) (panel a). Of note is the flux from the CD symmetric mode to the bending (and also to the umbrella) mode (panel c). Therefore, the modes do not maintain adiabaticity previous to the interaction of reactants.

Both CD asymmetric (ν_1 = 1, panel b) and CD symmetric (ν_2 = 1, panel c) excited modes are fast deactivated ($t \approx$ 0.4 and 0.2 ps, respectively), transferring energy to the lowest modes, and so the energy deposited in the two modes tends to be similar. Therefore, a part of the energy originally deposited into the CD stretch modes flows to the lowest modes, thus losing its potential efficiency. Consequently, the vibrational adiabaticity will not be preserved during the reactive process, or in other words, this reaction does not exhibit clear mode selectivity. Therefore, the presence of various degrees of vibrational

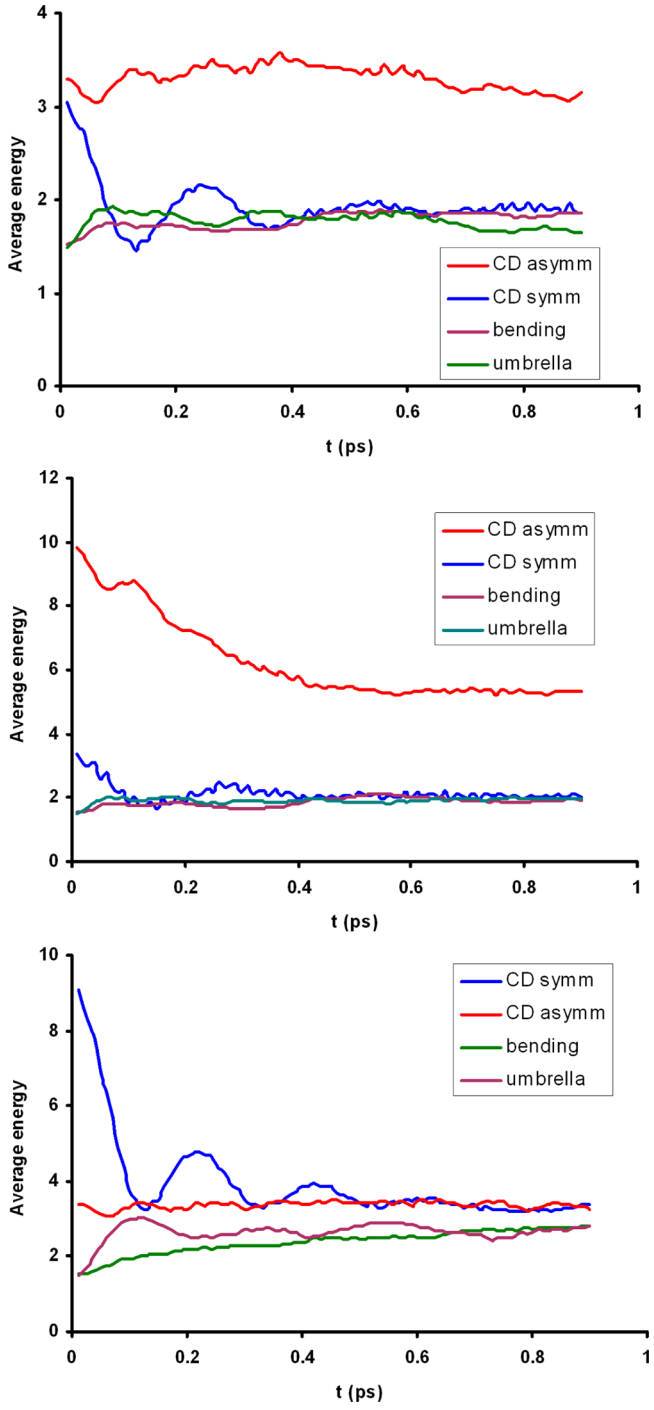

Figure 7. Average energy (kcal mol^{-1}) of each normal mode from QCT calculations as a function of time. Panel a shows the results for the vibrational ground state; panel b for excitation of the CD asymmetric stretching mode by one quantum, ν_1 = 1; and panel c for excitation of the CD symmetric stretching mode by one quantum, ν_2 = 1.

freedom in polyatomic systems, where IVR is possible, complicates the naïve picture of coupling terms.

Before finishing this section, we comment some limitations relating to the classical IVR analysis performed, which do not modify the main conclusions reached. First, the IVR time scale cannot be compared with the time scale for the QCT trajectories because in the IVR case the initial conditions (reactants distance and impact parameter) are set to ensure that

dx.doi.org/10.1021/jp502414e | J. Phys. Chem. A 2014, 118, 3572−3579

no reaction occurs (section 3.3). Second, the energy initially deposited into a vibrational mode flows to different modes much faster than it should, which is a known error in IVR analysis when classical trajectories are used. Third, this correlation between classical and quantum states is somewhat artificial since in this latter case the transfer of nonentire amounts of energy is forbidden. Having said this, it is also true that the wave function can be a superposition of several eigenstates, and thus, the presence of an excited state is probable even though there is not sufficient energy to excite it.

4.4.2. OD Vibrational Distribution. Before beginning this analysis, it may be illustrative to comment on the simpler H + $H_2O \rightarrow H_2$ + OH reaction, which is a textbook example. When one excites one of the OH bonds of water, the OH product appears in its vibrational ground-state, while when one excites the two OH bonds, the OH product appears vibrationally excited, $v = 1$. Only in this case, the initial vibrational excitation in the nonreactive OH bond of water survives the process and appears in the product.

For the $O(^3P)$ + $CD_4(\nu)$ reaction the OD(ν) vibrational distributions at collision energy of 15.0 kcal mol^{-1} are listed in Table 3, using the HB-All and 1GB approaches. On the basis of the PES-2014 surface, the 0 K reaction enthalpy is 3.1 kcal mol^{-1}, and the ω(OD) = 2760 cm^{-1} (~7.9 kcal mol^{-1}). Thus, the energy threshold to populate the first vibrational state of the OD product [OD($\nu = 1$)] is 11.0 kcal mol^{-1}. Therefore, with collision energy of 15.0 kcal mol^{-1} there is sufficient energy to populate this state. We begin by analyzing the $CD_4(\nu = 0)$ vibrational ground-state. Using the HB approach we find 34% of OD($\nu = 1$), while using the 1GB approach this percentage diminishes to 12%. At this collision energy, Czako et al.[10] reported 0% of population using the CB surface and the 1GB approach, while Zhang and Liu[12] obtained experimentally 15% (at collision energy of 12.49 kcal mol^{-1}). In sum, PES-2014 with the 1GB approach reproduces the experimental evidence, and the standard HB-All histogram binning overestimates the population of the OD($\nu = 1$) due to violation of the ZPE, i.e., artificial transfer of energy between products. Therefore, we shall use the 1GB approach for the remainder of this discussion.

Table 3. OD(ν) Vibrational Distributions at Collision Energy of 15.0 kcal mol^{-1} on the PES-2014 Surface for the $O(^3P)$ + $CD_4(\nu)$ Reaction

$CD_4(\nu)$	HB-All		1GB	
state	$\nu = 0$	$\nu = 1$	$\nu = 0$	$\nu = 1$
ground-state	64	34	88	12
asymm. stretch	44	48	40	60
symm. stretch	54	46	50	50
bending	61	37	74	26
umbrella	89	41	78	22

When the different $CD_4(\nu)$ vibrational modes are independently excited, $CD_4(\nu_i = 1, i = 1{-}4)$, the OD($\nu = 1$) product appears more vibrationally excited, proportional to the extra energy added by each mode, from 6.5 kcal mol^{-1} for the stretching asymmetric mode to 2.9 kcal mol^{-1} for the umbrella mode. Thus, the population in OD($\nu = 1$) depends on the CD_4 reactant vibrational mode excited and therefore on its energy: $\nu_1 \approx \nu_2 > \nu_3 \approx \nu_4$. The product vibrational excitation yielded by the CD stretch modes and the umbrella mode can be interpreted by using the reaction path curvature (eq 2) already analyzed in section 4.2 because of their coupling to the reaction path. The effect of the bending mode can be explained by using the coupling between modes (eq 4), where part of the energy initially deposited in this mode can flow to the umbrella mode.

With respect to the issue of mode selectivity, the vibrational excitation initially prepared in the reactive CD mode ($\nu_2 = 1$), which is broken in the reaction, only partially survives the reaction, OD($\nu = 1$), 50%, while the excitation of the other CD mode ($\nu_1 = 1$) yields even more OD excitation, 60%. Therefore, mode selectivity is not present (or only partially present) in this reaction.

4.5. Translational versus Vibrational Energy. As was noted in the Introduction, because of the larger number of vibrational modes present, the application of Polanyi's rules in polyatomic systems is not so straightforward as in atom + diatom reactions. Moreover, for central barrier reactions it is not clear how to apply these venerable rules.

For the $O(^3P)$ + CD_4 reaction, which presents a central barrier, the effects of equal amounts of energy as vibration or translation are studied. Note that in this study, we consider the CD asymmetric and symmetric stretch modes (ν_1 = 2295 cm^{-1} and ν_2 = 2074 cm^{-1}) and the CD_4 bending modes (ν_3 = 1060 cm^{-1} and ν_4 = 1011 cm^{-1}) in an independent way, at total energy of 15.0 kcal mol^{-1}. Thus, the combinations of translational and vibrational energy used can be seen in Table 4, where the CD_4 rotational energy does not appear, although obviously it is included in the QCT calculations.

Table 4. Combinations of Translational and Vibrational Energies

	E_{coll} (kcal mol^{-1})	E_{vib} (kcal mol^{-1})	E_{total} (kcal mol^{-1})
O + $CD_4(\nu = 0)$	15.0	0.0	15.0
O + $CD_4(\nu_1 = 1)$	8.5	6.5	15.0
O + $CD_4(\nu_2 = 1)$	9.1	5.9	15.0
O + $CD_4(\nu_3 = 1)$	12.0	3.0	15.0
O + $CD_4(\nu_4 = 1)$	12.1	2.9	15.0

The reaction probability ratios are listed in Table 5. First, for an equal amount of energies, translational energy is more effective than vibrational energy. These results agree with the QCT results reported by Czako et al.[10,11] using a different PES. Second, this behavior is strongly dependent on the mode excited. Thus, the effect of the ν_1 (asymmetric CD stretch) or ν_2 (symmetric CD stretch) modes is twice that of the ν_3 (bending) or ν_4 (umbrella) modes. Therefore, the vibrational excitation of the stretching modes is more efficient than the vibrational excitation of the bending modes. Note that this was suggested by our analysis of the effect of the vibrational excitation on the reactivity (Table 2). For purposes of comparison, we have also included in Table 5 results with the HB-DZPE correction. We find that HB-DZPE diminishes the P_t/P_v relationship and that it even inverts the tendency for the bending modes, i.e., the vibrational excitation is more effective than translational energy. However, it is necessary to note that the HB-DZPE correction treats differently the ground-state and the vibrational excitations, overestimating the effect of the vibrational excitations. So, the HB-DZPE constraint is more severe for the ground-state than for the vibrational excitations, with more trajectories discarded in the first case. Therefore, for this comparison the HB-DZPE constraint is less realistic than when all trajectories are considered.

dx.doi.org/10.1021/jp502414e | J. Phys. Chem. A 2014, 118, 3572−3579

Table 5. Ratio of Reaction Probabilities,[a] on the PES-2014 Surface, for Different Translational and Vibrational Energy[b] Combinations

vibration	translation	total	P_t/P_v[c]
E_{total} =15.0 kcal mol^{-1}			
$\nu = 0$	15.0	15.0	1
$\nu_1 = 1$	8.5	15.0	4.91 (2.00)
$\nu_2 = 1$	9.1	15.0	2.27(1.26)
$\nu_3 = 1$	12.0	15.0	1.53(0.86)
$\nu_4 = 1$	12.1	15.0	1.49(0.86)
Another Total Energy (kcal mol^{-1})			
$\nu = 0$	21.5	21.5	
$\nu_1 = 1$	15.0	21.5	1.54 (0.64)
$\nu = 0$	20.9	20.9	
$\nu_2 = 1$	15.0	20.9	1.35 (0.67)
$\nu = 0$	18.0	18.0	
$\nu_3 = 1$	15.0	18.0	1.27 (0.73)
$\nu = 0$	17.9	17.9	
$\nu_4 = 1$	15.0	17.9	1.42 (0.79)

[a]All vibrational states of the products have been considered. [b]Energies in kcal mol^{-1}. [c]Values using the HB-All approach; in parentheses, using the HB-DZPE approach. Maximum error bar ±0.1.

To confirm these points, we performed a second set of trajectories at higher total energies, which are also listed in Table 5. Now the possible combinations can be seen in Table 6.

Table 6. Combinations of Translational and Vibrational Energies

	E_{coll} (kcal mol^{-1})	E_{vib} (kcal mol^{-1})	E_{total} (kcal mol^{-1})
O + $CD_4(\nu = 0)$	21.6	0.0	21.6
O + $CD_4(\nu_1 = 1)$	15.0	6.5	21.6
O + $CD_4(\nu = 0)$	20.9	0.0	20.9
O + $CD_4(\nu_2 = 1)$	15.0	5.9	20.9
O + $CD_4(\nu = 0)$	18.0	0.0	18.0
O + $CD_4(\nu_3 = 1)$	15.0	3.0	18.0
O + $CD_4(\nu = 0)$	17.9	0.0	17.9
O + $CD_4(\nu_4 = 1)$	15.0	2.9	17.9

As before, CD_4 rotational energy is included in the QCT calculations, although it does not appear here. We find the same behavior as at lower energies, but more pronounced. Now, using the HB-DZPE constraint the vibrational excitation is more effective than translational energy for all vibrational modes of $CD_4(\nu)$. Therefore, the HB-DZPE constraint is too restrictive, and it cannot be used in this case.

In sum, while for late and early barriers the effects of vibrational and translational energy are straightforward to predict, (especially in the case of atom + diatom reactions), for reactions with central barrier, as that studied in the present article, the venerable Polanyi's rules are not of application.

5. CONCLUSIONS

We describe detailed QCT calculations of the $O(^3P) + CD_4(\nu)$ reaction using a full-dimensional analytical potential energy surface and analyze the role of vibrational excitations and translational energy on reactivity.

1. With respect to the vibrational ground-state, all vibrational excitations of $CD_4(\nu_i = 1, i = 1-4)$ enhanced reactivity by factors ~2.0−1.3, where the CD stretching modes had a more substantial effect.
2. Analysis of mode selectivity for this reaction showed that the vibrational excitation of the reactive mode (CD stretching mode, which is broken in the reaction), was partially maintained in the OD product and that the independent vibrational excitations of the CD asymmetric and symmetric stretch modes showed similar reactivity and OD product vibrational populations. These results suggest partial or negligible mode selectivity, which is related with fast IVR during the reaction.
3. In order to study the relative efficiency of equal amounts of energy as vibration or translation in surmounting this central barrier reaction, the QCT results show that the translational energy raises the reactivity more effectively than the vibration energy. As Polanyi did not study the central barrier reactions, it is unclear how to apply these rules to this polyatomic reaction. In addition, the larger number of vibrational modes than in atom−diatom reactions complicate the analysis.

In sum, these QCT calculations show that the spectrator model is a very naïve picture to describe this reaction, which exhibits only partial or negligible mode selectivity, and where the Polanyi's rules are not applicable. We found that this behavior is related to strong couplings between vibrational modes and with the reaction coordinate. Obviously, these conclusions depend on the reliability of the potential energy surface, the limitations of the classical nature of the QCT calculations, and the harmonic approach used in the normal-mode analysis. However, it is interesting to note that all the results point in the same direction, which lends confidence to these conclusions.

Bond selectivity and mode selectivity are issues widely studied in dynamics, and Simons[27] noted that they are events in chemistry, i.e., they are the exception and not the rule.

AUTHOR INFORMATION

Corresponding Author

*E-mail: joaquin@unex.es.

Notes

The authors declare no competing financial interest.

ACKNOWLEDGMENTS

This work was partially supported by Gobierno de Extremadura, Spain, and Fondo Social Europeo (Project No. IB10001). Many calculations were carried out on the LUSITANIA computer at Computaex (Spain). We thank Prof. Kopin Liu for the experimental data to plot Figure 6 and the TOC.

REFERENCES

(1) Polanyi, J. C. Concepts in Reaction Dynamics. *Acc. Chem. Res.* **1972**, *5*, 161−168.

(2) Nesbitt, D. J.; Field, R. W. Vibrational Energy Flow in Highly Excited Molecules: Role of Intramolecular Vibrational Redistribution. *J. Phys. Chem.* **1996**, *100*, 12735−12756.

(3) Monge-Palacios, M.; Espinosa-Garcia, J. Role of Vibrational and Translational Energy in the OH + NH_3 Reaction: A Quasi-Classical Trajectory Study. *J. Phys. Chem. A* **2013**, *117*, 5042−5051.

(4) Monge-Palacios, M.; Corchado, J. C.; Espinosa-Garcia, J. Quasi-Classical Trajectory Study of the Role of Vibrational and Translational Energy in the Cl + NH_3 Reaction. *Phys. Chem. Chem. Phys.* **2012**, *14*, 7497−7508.

(5) Espinosa-Garcia, J. Vibrational versus Translational Energies in the F + CH_4 Reaction: A Comparison with the F + CH_2D_2 Reaction Using Quasi-Classical Trajectory Methods. *Chem. Phys. Lett.* **2010**, *488*, 153−157.
(6) Espinosa-Garcia, J. Quase-Classical Trajectory Calculations Analyzing the Role of Vibrational and Translational Energy in the F + CH_2D_2 Reaction. *J. Chem. Phys.* **2009**, *130*, 054305.
(7) Yan, S.; Wu, Y.-T.; Zhang, B.; Yue, X.-F.; Liu, K. Do Vibrational Excitations of CHD_3 Preferentially Promote Reactivity Toward the Chlorine Atom? *Science* **2007**, *316*, 1723−1726.
(8) Corchado, J. C.; Truhlar, D. G.; Espinosa-Garcia, J. Potential Energy Surface, Thermal and State-Selected Rate Coefficients, and Kinetic Isotope Effects for Cl + CH_4. *J. Chem. Phys.* **2000**, *112*, 9375−9389.
(9) Sanson, J.; Corchado, J. C.; Rangel, C.; Espinosa-Garcia, J. Quasi-Classical Trajectory Calculations Analyzing the Role of Bending Mode Excitations of Methane in the Cl + CH_4 Reaction. *J. Phys. Chem. A* **2006**, *110*, 9568−9574.
(10) Czakó, G.; Liu, R.; Yang, M.; Bowman, J. M.; Guo, H. Quasiclassical Trajectory Studies of the $O(^3P)$ + $CX_4(v_k = 0, 1)$ → $OX(v)$+ $CX_3(n_1n_2n_3n_4)$ [X = H and D] Reactions on an ab Initio Potential Energy Surface. *J. Phys. Chem. A* **2013**, *117*, 6409−6420.
(11) Liu, R.; Yang, M.; Czako, G.; Bowman, J. M.; Li, J.; Guo, H. Mode Selectivity for a "Central" Barrier Reaction: Eight-Dimensional Quantum Studies of the $O(^3P)$ + CH_4 → OH + CH_3 Reaction on an Ab Initio Potential Energy Surface. *J. Phys. Chem. Lett.* **2012**, *3*, 3776−3780.
(12) Zhang, B.; Liu, K. How Active Is the Bend Excitation of Methane in the Reaction with O (^3P). *J. Phys. Chem. A* **2005**, *109*, 6791−6795.
(13) Wang, F.; Liu, K. Enlarging the reactive cone of acceptance by exciting the C−H bond in the $O(^3P)$ + CHD_3 reaction. *Chem. Sci.* **2010**, *1*, 126−133.
(14) Liu, K. Personal communication.
(15) Jiang, B.; Guo, H. Relative Efficacy of Vibrational vs. Translational Excitation in Promoting Atom-Diatom Reactivity: Rigorous Examination of Polanyi's Rules and Proposition of Sudden Vector Projection (SVP) Model. *J. Chem. Phys.* **2013**, *138*, 234104.
(16) Liu, J.; Song, K.; Hase, W. L.; Andersen, S. L. Direct Dynamics Trajectory Study of Vibrational Effects: Can Polanyi Rules be Generalized to a Polyatomic System? *J. Am. Chem. Soc.* **2004**, *126*, 8602−8603.
(17) Gonzalez-Lavado, E.; Corchado, J. C.; Espinosa-Garcia, J. The Hydrogen Abstraction Reaction $O(^3P)$ + CH_4. A New Analytical Potential Energy Surface Based on Fit to ab Initio Calculations. *J. Chem. Phys.* **2014**, *140*, 064310.
(18) Czako, G.; Bowman, J. L. Dynamics of the O+ CH_3D Reactions on an Accurate Ab initio Potential Energy Surface. *Proc. Natl. Acad. Sci. U.S.A.* **2012**, *109*, 7997−8001.
(19) Hase, W. L.; Duchovic, R. J.; Hu, X.; Komornicki, A.; Lim, K. F.; Lu, D.-H.; Peslherbe, G. H.; Swamy, K. N.; Van de Linde, S. R.; Varandas, A. J. C.; Wang, H.; Wolf, R. J. VENUS96: A General Chemical Dynamics Computer Program. *QCPE Bull.* **1996**, *16*, 43.
(20) Hu, X.; Hase, W. L.; Pirraglia, T. Vectorization of the General Monte Carlo Classical Trajectory Program VENUS. *J. Comput. Chem.* **1991**, *12*, 1014−1024.
(21) Bonnet, L. The Method of Gaussian Weighted Trajectories. III. An Adiabaticity Correction Proposal. *J. Chem. Phys.* **2008**, *128*, 044109−044115.
(22) Czakó, G.; Bowman, J. M. Quasiclassical Trajectory Calculations of Correlated Product Distributions for the F + CHD_3 (v_1 = 0, 1) Reactions Using an ab Initio Potential Energy Surface. *J. Chem. Phys.* **2009**, *131*, 244302 (19 pages).
(23) Truhlar, D. G.; Blais, N. C. Legendre Moment Method for Calculating Differential Scattering Cross Sections from Classical Trajectories with Monte Carlo Initial Conditions. *J. Chem. Phys.* **1977**, *67*, 1532−1539.
(24) Corchado, J. C.; Espinosa-Garcia, J. Product Vibrational Distributions in Polyatomic Species Based on Quasiclassical Trajectory Calculations. *Phys. Chem. Chem. Phys.* **2009**, *11*, 10157−10164.
(25) Miller, W. H.; Handy, N. C.; Adams, J. E. Reaction Path Hamiltonian for Polyatomic Molecules. *J. Chem. Phys.* **1980**, *72*, 99−112.
(26) Kraka, E.; Dunning, T. H. Characterization of Molecular Potential Energy Surfaces: Critical Points, Reactions paths and Reaction Valleys. In *Advances in Molecular Electronic Structure Theory*; JAI: New York, 1990; Vol. *1*, pp 129−173.
(27) Simons, J. P. Spiers Memorial Lecture Stereochemistry and Control in Molecular Reaction Dynamics. *Faraday Discuss.* **1999**, *113*, 1−25.